INTER-NOISE 2006
3-6 DECEMBER 2006
HONOLULU, HAWAII, USA

Tracking energy flow using a Volumetric Acoustic Intensity Imager (VAIM)

Earl G. Williams [1]and Nicolas P. Valdivia[2]
Acoustics Division,
Naval Research Laboratory,
Washington, DC 20375-5320, USA.

Jacob Klos[3]
Structural Acoustics Branch,
NASA Langley Research Center,
Hampton, VA 23681-2199, USA

ABSTRACT

A new measurement device has been invented at the Naval Research Laboratory which images instantaneously the intensity vector throughout a three-dimensional volume nearly a meter on a side. The measurement device consists of a nearly transparent spherical array of 50 inexpensive microphones optimally positioned on an imaginary spherical surface of radius 0.2m. Front-end signal processing uses coherence analysis to produce multiple, phase-coherent holograms in the frequency domain each related to references located on suspect sound sources in an aircraft cabin. The analysis uses either SVD or Cholesky decomposition methods using ensemble averages of the cross-spectral density with the fixed references. The holograms are mathematically processed using spherical NAH (nearfield acoustical holography) to convert the measured pressure field into a vector intensity field in the volume of maximum radius 0.4 m centered on the sphere origin. The utility of this probe is evaluated in a detailed analysis of a recent in-flight experiment in cooperation with Boeing and NASA on NASA's Aries 757 aircraft. In this experiment the trim panels and insulation were removed over a section of the aircraft and the bare panels and windows were instrumented with accelerometers to use as references for the VAIM. Results show excellent success at locating and identifying the sources of interior noise in-flight in the frequency range of 0 to 1400 Hz. This work was supported by NASA and the Office of Naval Research.

1 INTRODUCTION

The intension of this paper is to demonstrate the capability of the VAIM to separate acoustical sources and display the vector intensity associated with each. The sources may

[1]Email address: williams@pa.nrl.navy.mil
[2]Email address: valdivia@pa.nrl.navy.mil
[3]Email address: j.klos@nasa.gov

be random in nature and may be correlated, partially correlated, or uncorrelated with one another. To do this we turn to a recent experiment on the bare sidewall of a Boeing 757 aircraft. This particular experiment assessed the quieting effects of different sidewall treatments, and the bare sidewall case provided the baseline for estimating the transmission loss of various treatments. The bare sidewall measurements provided an ideal forum for testing the VAIM, as our spherical array "passenger" was not shielded by sidewall trim panels and insulation, providing a high correlation environment for testing. A recent paper discusses the VAIM in detail[1] and we will not repeat the discussion here.

2 EXPERIMENT DESCRIPTION & PROCESSING

The NASA research plane used is shown in Fig. 1 along with the arrangement in the interior used for the experiment. The aircraft was flown at a controlled altitude of 30 000 feet at a constant speed of 0.8 M. In the interior in the forward section of the aircraft the insulation and trim panels was removed from 4 sidewall sections (bays). A 120 element conformal array is shown, which is not discussed in this paper, as well as the 50 microphone spherical array. A closeup picture of the spherical array is shown in Fig. 2. The radius of the array is 0.2 m and it was located nominally with its origin at 0.4 m from the skin of the fuselage sidewall. Note that the origin of the array is directly in front of a window. Figure 1 also shows the locations of most of the reference accelerometers (some circled for clarity) which were attached to the fuselage sidewall panels and to the windows. A total of 31 accelerometers were used. All of the panels in the 3 sections were monitored with attached accelerometers. Most of the seats throughout the aircraft were removed. The 50

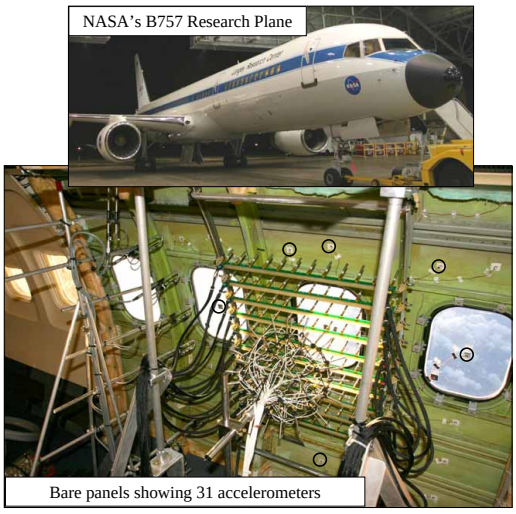

Figure 1: NASA's Aries 757 aircraft and the interior showing the four stripped bays. 31 accelerometers were attached throughout the 3 bays on the right. Some of the accelerometers are circled for clarity.

microphones and 31 accelerometers were all sampled simultaneously for 20 min at 12 000 samples/s and recorded digitally on tape for processing later. More information about the experiment can be found in a Noise-Con paper.[2] Back in the laboratory the tapes were

Figure 2: 50 element spherical array designed and constructed at NRL, shown in the laboratory for structural acoustics at NRL.

read and the data processed. For this data set we partitioned the time data into 2048 point segments and used FFT's to convert to the frequency domain. Cross and auto correlations were performed on the 81 channels of data using ensemble averaging consisting of a total of 1200 ensembles representing about 3 min of data out of the available 20 minutes.

2.1 Preliminary data analysis

The large volume of measured data can be organized efficiently to set the stage for a clear, coherent analysis by the VAIM for uncovering dominant acoustic sources and displaying their vector intensity fields. Probably the most important preliminary result is the autospectral density of the calibrated accelerometers. This result is shown in Fig. 3 with the power spectral density (PSD) color coded in a 70 dB range. On the vertical axis is frequency (the bin size was about 6 Hz) and the horizontal axis is the accelerometer number. The legend for the location of these accelerometers is shown to the left in the figure with the individual panels and widows indicated with grey lines. Note that the order of the references along the horizontal axis is organized so that accelerometers in a row are grouped together. An attempt to clarify this ordering is shown in the rotated reference location picture shown above the PSD color plot. Thus PSD data near the origin of the plot corresponds to the top accelerometers (i.e. near the luggage storage areas above a passenger), and the data to the far right corresponds to references mounted on panels near the floor of the aircraft. As one might expect there is a dramatic difference in the vibration in the widow regions versus the skin panels. The dark red areas indicate high responses of the panels probably due to resonances excited by the turbulent flow outside the aircraft. Although most of the individual panels are the same width, they are attached to the the vertical frames differently. The horizonal longerons can been also seen. They are riveted directly to all the panels. The lower panels are riveted additionally to the vertical frames, whereas the upper panels are not and pass under these frames without touching. As a result of this attachment a set of well defined resonances appear in the lower panels as can be seen in Fig. 3. The upper panels which because they are unattached are much longer display a more muted resonance character. Of course some resonances may be missed, as many of the accelerometers are attached to the center of the panel, and any modes with nodal lines at the panel center will not appear in the

PSD. Finally the longeron just below the window is different in structure than the longerons framing the panels containing accelerometers numbers 5,6,16,17,27 and 28 resulting in a different resonance structure of the panels just below the window (accelerometers 4,9,..., 26 and 31). In the figure the x's have indicate the accelerometer with the highest partial coherence to the microphones, as will be described later.

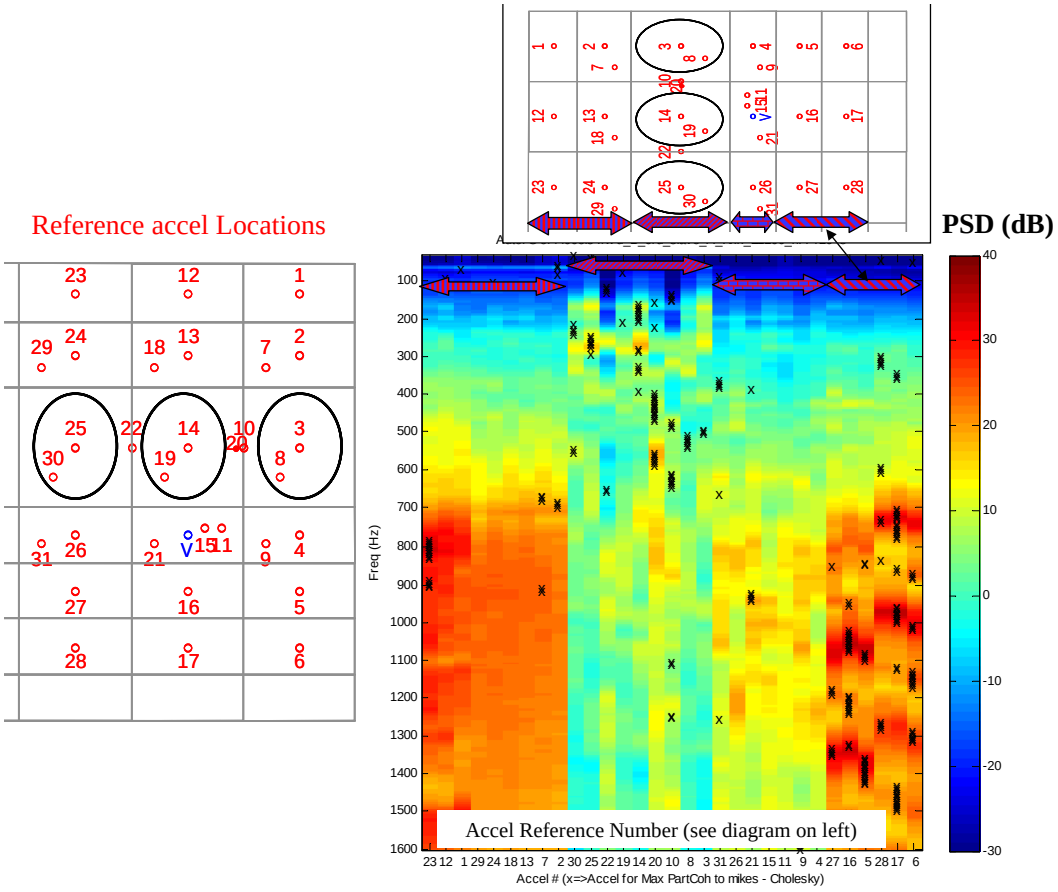

Figure 3: Auto power spectra (70 dB range) of the 31 accelerometers. The key on the left indicates the numbered accelerometer locations in the three adjacent bays corresponding to the numbers on the horizontal axis of the plot.

In Fig. 4 the average sound pressure level (SPL) measured by the 50 microphones is shown using an A weighted scale. The red curve is the SPL and the blue curve (using the scale on the right) will be described later. As can be seen the levels are quite high due to lack of trim panels and insulation on the fuselage sidewall.

2.2 Signal processing overview

The signal processing for the creation of partial field holograms was first developed by Jrgen Hald and extended by Stuart Bolton.[3, 4, 5] The ensemble averaging used is defined

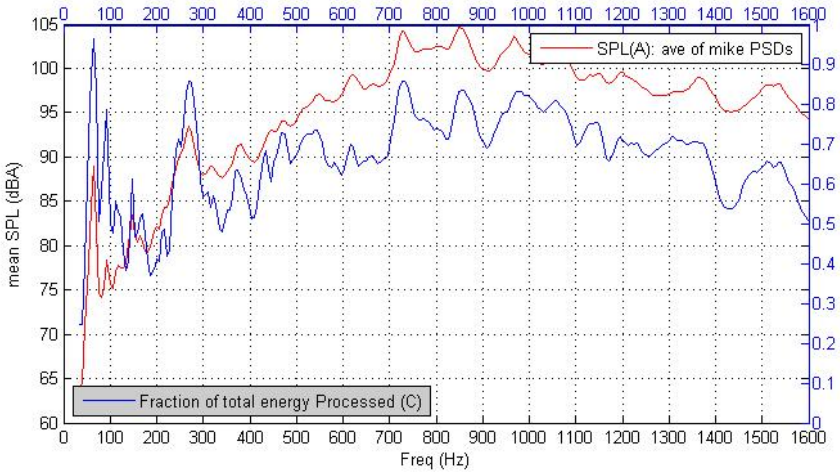

Figure 4: Average auto power spectra measured by the 50 microphones converted to an A weighted sound pressure level.

by $S_{x_ip_j} = \bar{\mathcal{E}}[X_i{}^*(f)P_j(f)]$ and $S_{x_ix_j} = \bar{\mathcal{E}}[X_i{}^*(f)X_j(f)]$ each representing terms of a cross-spectral matrix. Here X_i is the ith reference accelerometer ($1 \le i \le 31$) and P_j the jth microphone in the array ($1 \le j \le 50$). In the data presented in this paper we use a 2048 point FFT of the time series (sample rate was 12kHz) and the ensemble average consists of 1200 overlapping (50%) ensembles. Each ensemble was 0.17 s in length. We compute the average coherence of ith reference to each of the 50 microphones,

$$\overline{\gamma^2_{x_ip}} \equiv \frac{1}{50}\sum_{j=1}^{50}\gamma^2_{x_ip_j}, \tag{1}$$

where the coherence is defined as usual by $\gamma^2_{x_ip_j} = |S_{x_ip_j}|^2/(S_{x_ix_i}S_{p_jp_j})$.

From Eq. (1) we can determine which references are important with respect to the field measured at the microphone locations. We rank the references by average coherence using $\overline{\gamma^2_{x_mp}} > \overline{\gamma^2_{x_np}} > \cdots > \overline{\gamma^2_{x_kp}}$, and order the two cross-spectral density matrices, $\mathbf{S_{xx}}$ and $\mathbf{S_{xp}}$, (done at each frequency) yielding

$$\mathbf{S_{xx}} \equiv \begin{pmatrix} S_{x_mx_m} & S_{x_mx_n} & \cdots & S_{x_mx_k} \\ S_{x_nx_m} & S_{x_nx_n} & \cdots & S_{x_nx_k} \\ \vdots & \vdots & \ddots & \vdots \\ S_{x_kx_m} & S_{x_kx_n} & \cdots & S_{x_kx_k} \end{pmatrix}^{31\times 31} = \underbrace{\mathbf{T}^H\mathbf{T}}_{\text{Cholesky}} \tag{2}$$

$$\mathbf{S_{xp}} \equiv \begin{pmatrix} S_{x_mp_1} & S_{x_mp_2} & \cdots & S_{x_mp_{50}} \\ S_{x_np_1} & S_{x_np_2} & \cdots & S_{x_np_{50}} \\ \vdots & \vdots & \ddots & \vdots \\ S_{x_kp_1} & S_{x_kp_2} & \cdots & S_{x_kp_{50}}. \end{pmatrix}^{31\times 50} \tag{3}$$

The ordered $\mathbf{S_{xx}}$ matrix in Eq. (2) is decomposed into a product of an upper triangular matrix $\mathbf{T}$ and its conjugate transpose $\mathbf{T}^H$, a Cholesky decomposition. The partial field

holograms are finally determined in the standard way[1] from

$$\begin{pmatrix} P_{x_m p_1} & P_{x_m p_2} & \cdots & P_{x_m p_{50}} \\ P_{x_n p_1} & P_{x_n p_2} & \cdots & P_{x_n p_{50}} \\ \vdots & \vdots & \ddots & \vdots \\ P_{x_k p_1} & P_{x_k p_2} & \cdots & P_{x_k p_{50}} \end{pmatrix}^{31\times 50} = (\mathbf{T}^H)^{-1}\mathbf{S_{xp}}. \tag{4}$$

The 31 rows of Eq. (4) each represent a partial field hologram, that is, each row contains 50 complex pressures (phased holograms) related to a specific reference. The first row extracts the pressure field related to reference number m. Due to the characteristics of the Cholesky decomposition each successive row represents the complex field related to the indicated reference with the effects of all the references in the rows above removed.[6] This is a critical aspect of the decomposition. For example assume that reference m (1st row) and n (2nd row) are correlated somewhat to one another. The Cholesky decomposition removes the correlated part of n in the the complex pressure represented by the second row of the matrix. Correspondingly, the Cholesky processing leaves the 3rd row uncorrelated to the 1st and 2nd, and so on. This procedure reflects an orthogonalization process of correlation. A bit of reflection reveals that the ordering of the reference matrix in Eq. (2) is crucial, especially when dealing with partially correlated references.

An important figure of merit is the fraction of the total signal energy represented by one of the partial holograms at a particular frequency. The total signal energy at a microphone location j is given by autospectral density $S_{p_j p_j}$ and the signal energy represented by the partial field of the ith reference (ith row of the matrix) given in Eq. (4) is $|P_{x_i p_j}|^2$. If we average over all 50 microphones,

$$\Gamma_i^2 = \frac{1}{50}\sum_{j=1}^{50}\frac{|P_{x_i p_j}|^2}{S_{p_j p_j}} \tag{5}$$

we have in Γ_i^2 a measure of the fraction of the total signal energy represented by the ith partial field. The relation $\Gamma_i^2 \leq 1$ always holds. Γ_i^2 is also called the partial (or virtual) coherence. The importance of Γ_i^2 is that it indicates how much of the total measured pressure signal is related to the ith reference. The sum $\Gamma^2 = \sum_{i=1}^{31}\Gamma_i^2$ over the reference set gives a measure of how much of the total signal energy is represented by the set of chosen references. References that are placed on sources that do not contribute to the sound field in the region of the sphere will be indicated by $\Gamma_i^2 \approx 0$, and conversely a dominant source that is monitored by a reference transducer would be indicated by $\Gamma_i^2 \approx 1$.

Now we can return to Fig. 4 and note that the blue curve labeled "Fraction of total energy Processed (C)" represents the defined quantity Γ^2, and the corresponding vertical axis is shown on the right (values 0 to 1). We see that the fraction of the total energy related to the 31 references varies from about 40% (0.4) to nearly 100% for one low frequency peak. Over most of the frequency range more than 60% of the energy has been accounted for by the reference set. It is interesting to note, although the experiment was not discussed here, that when the 4 bare sidewall panels are covered with damping treatment this fraction drops to below 15% over most of the frequency range for the same reference set.

The final step in our analysis is to determine where the sources are that contribute significantly to our spherical "passenger".

3 VECTOR INTENSITY RECONSTRUCTIONS

First we consider the peak in the SPL curve of Fig. 4 at 269 Hz. We can see that the SPL reached a level of about 93 dB(A) and the energy fraction of the total measured field represented by the 31 references was about 0.85 or 85%. Figure 5 shows the vector intensity reconstruction at 269 Hz, reconstructed using spherical NAH[1] from the first row of Eq. (4) and represents the partial hologram related to reference number 25 (window mounted accelerometer). The vector intensity pattern is shown by the red cones who's size

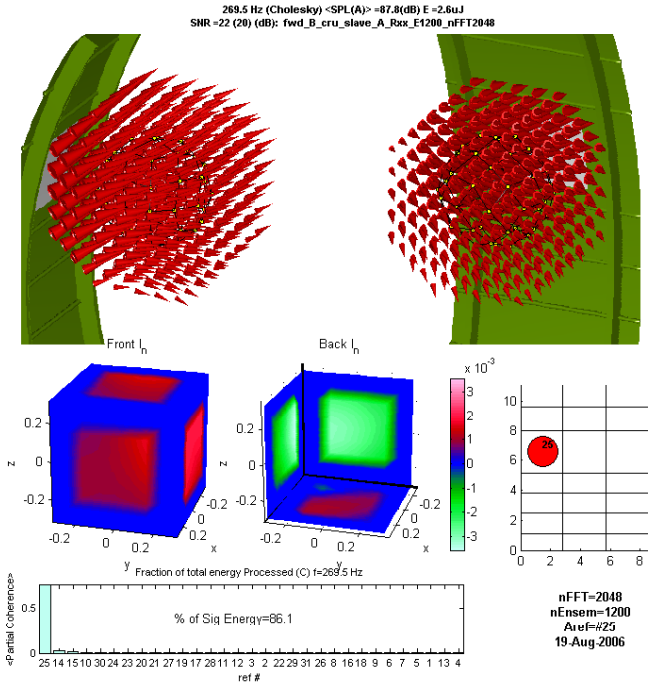

Figure 5: Vector intensity result from the VAIM measurement at 269 Hz.

is proportional to the linear intensity. Two views of the field are shown to help identify the direction of the flow. The green background represents the bay in front of the VAIM. The cube in the figure below the vector plots represents the normal intensity on each of the 6 faces color coded so that green is intensity into the cube and red is intensity directed out of the cube. The strips of blue regions near the edges of the cube represent regions where $r > 0.4m$ and the intensity is not computed in this region. From this display it is very evident (top faces of the cube on right) that the direction of the energy flow is coming from the bay to the left of the one displayed in the vector display at the height of the array (the window in that bay specifically). The display to the right of the cubes indicates by a red dot the reference accelerometer location for this partial field. The bar plot at the bottom of the figure shows the average partial coherence (fraction of total energy) of all the

31 references, ordered from highest to lowest and numbered on the horizontal axis. In this case the average partial coherence $\Gamma^2_{25} = 0.76$, that is, 76% of the energy was related to the accelerometer on the window on the bay to the left of the bay directly in front of the array. The next strongest source has $\Gamma^2_{14} = 0.02$ (window in front of the array) and thus is relatively unimportant. Referring back to Fig. 3 one can see that the dominant accelerations occur in the window regions from 150-400 Hz indicating that the main mechanism at play here is resonances of the windows. The vector intensity confirms that they indeed are sources of noise for our spherical "passenger".

The next peak of significance in Fig. 4 is at 726 Hz. According to Fig. 3 it appears at this frequency that the lower panels of the 3 bays are in resonance (corresponding to attached accelerometers 6, 17 and 28). The first volumetric intensity from the first two partial fields is shown in Fig. 6. Indeed accelerometer 17 is attached to the dominant source with the highest fractional energy (54%) and one can see that the vector intensity field appears to originate below the sphere (appears to diffract parallel to the fuselage sidewall). The plot to the right in the figure is the second partial field which contains 10% of the total signal energy and is correlated with the accelerometer on the left bottom panel, accelerometer 28. It is important to note that the references for the first and second partial fields are fairly highly correlated to each other, with a coherence of about 0.7. As discussed above the Cholesky decomposition procedure attempts to orthogonalize the coherence between these two references, by extracting the part of accelerometer 28 that is uncorrelated to accelerometer 17. The partial field of the former is thus uncorrelated to the partial field of the latter. This appears to be a logical way to deal with partially correlated source fields that retains clarity of interpretation.

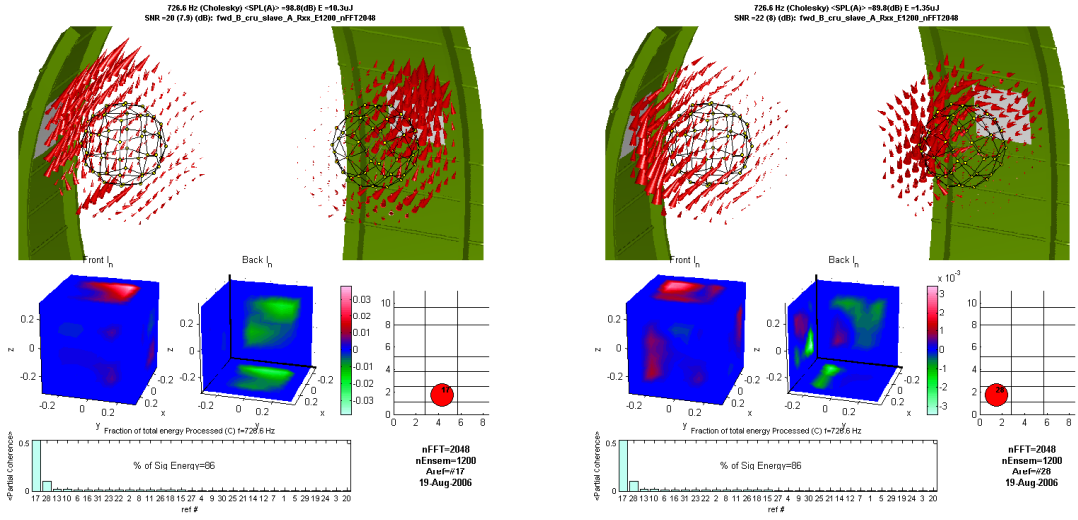

Figure 6: Vector intensity result for the first two partial fields from the VAIM measurement at 726 Hz.

In the final set of figures we look at a case where several uncorrelated panels contribute to the intensity field and are correctly separated by the VAIM. The results shown in Fig. 7 are for 803 Hz, a frequency at which both the upper and lower panels appear to be resonance according to Fig. 3. We display four partial fields for this case. The first two are shown

in Fig. 7 and the third and fourth in Fig. 8. The first partial field with 21% of the total

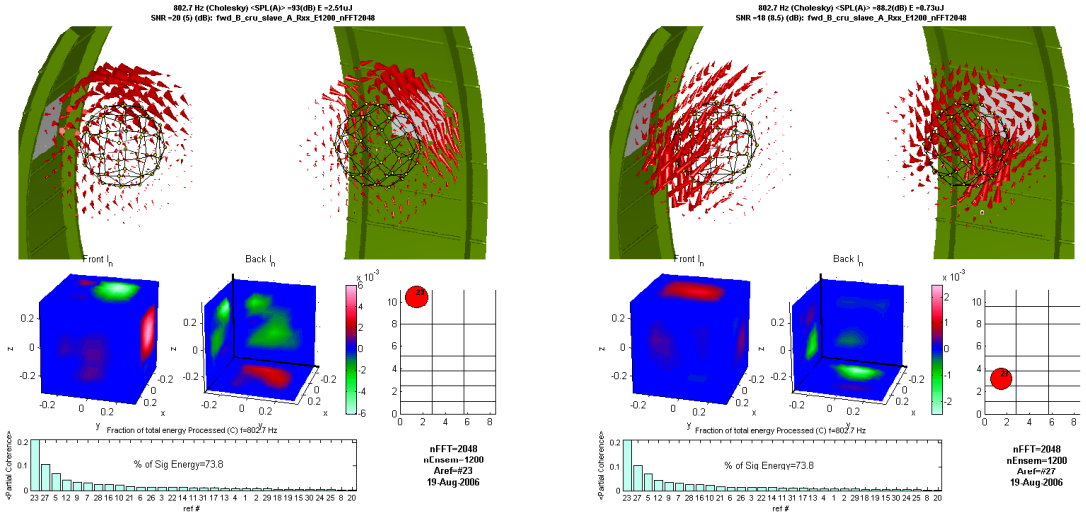

Figure 7: Vector intensity result for the first two partial fields from the VAIM measurement at 802 Hz.

signal energy correlates with accelerometer 23 on the very top left panel (near the ceiling of the fuselage). The turbulent flow for this source probably arises from a different mechanism that the flow exciting the lower panel, contributing to the second partial field shown at the right in the figure correlated with accelerometer 27, and representing about 11% of the signal energy. Again the intensity cubes help to identify the direction of the intensity flow. Note that the coherence between these two accelerometers was less than 0.1, indicating that the corresponding panels are almost uncorrelated to one another.

The third and fourth partial fields shown in Fig. 7 contain 7% and 4% of the measured total energy, and thus are minor contributors, yet are still clearly resolved by the VAIM. The partial fields displayed on the left and right are correlated with references 5 and 12, one on a lower fuselage panel and one on a high fuselage panel respectively. Again the volumetric intensity appears to originate at the panel corresponding to the reference indicated. The adjacent panels at the top (23 and 12) were highly correlated with a coherence over 0.8. But again it should be realized that the Cholesky approach has removed the coherent part of 12, and the field displayed arises from the uncorrelated part.

4 CONCLUSION

It has been demonstrated that the VAIM, through its images vector intensity fields, is able to locate sources of flow noise heard by the spherical "passenger" and is able to separate several sources at a given frequency and identify the vector fields associated with each. This is hoped to provide a demonstration of the utility of the VAIM for general noise source identification problems.

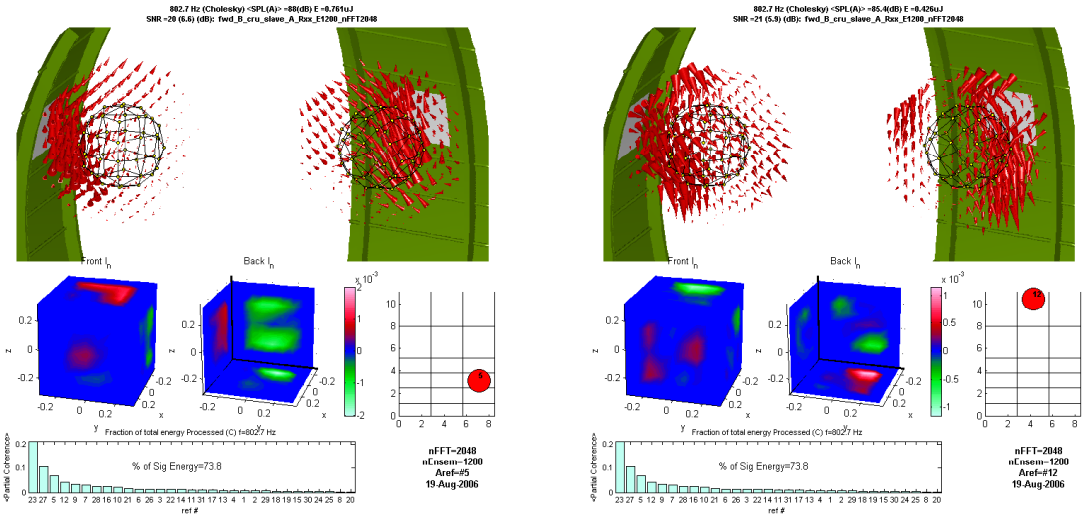

Figure 8: Vector intensity result for the third and fourth partial fields from the VAIM measurement at 802 Hz.

Acknowledgements

This work was supported by the Office of Naval Research. Experimental work and data analysis was supported by NASA Langley and The Boeing Company provided critical experiment support.

References

[1] Earl G. Williams, Nicolos P. Valdivia, Peter C. Herdic, and Jacob Kloss. Volumetric acoustic vector intensity imager. *J. Acoust. Soc. Am.*, 120:TBD, 2006.

[2] Jacob Klos and et. al. Comparison of different measurement technologies of the in-flight assessment of radiated acoustic intensity. In *Proceedings of Noise-Con 2005*, Minneapolis, Minnesota, October 2005.

[3] Jørgen Hald. STSF - a unique technique for scan-based nearfield acoustical holography without restriction on coherence. Technical report, B&K Technical Review, No. 1, 1989.

[4] D. L. Hallman and J. S. Bolton. Multi-reference nearfield acoustical holography. In *Proceedings Inter-noise '92*, pages 1165–1170, Toronto, Canada, July 1992.

[5] D. L. Hallman and J. S. Bolton. A comparison of multi-reference nearfield acoustical holography procedures. In *Proceedings Noise-Con '94*, pages 929–934, Ft. Lauderdale, Florida, May 1994.

[6] Julius S. Bendat and Allan G. Piersol. *Random Data Analysis and Measurement Procedures*. John Wiley & Sons, New York, NY, third edition, 2000.